Powder Neutron Diffraction Study of the Ordered Oxygen-Deficient Perovskites $(La,Sr)_8Cu_{8-x}Fe_xO_{20}$

R. Genouel, C. Michel,* and B. Raveau

Laboratoire Crismat, CNRS URA 1318, ISMRa / Université de Caen, Bd du Maréchal Juin, 14050 Caen Cedex France

Received June 12, 1995. Revised Manuscript Received September 13, 1995[⊗]

The structure of three tetragonal ordered oxygen deficient perovskites $(La,Sr)_8Cu_{8-x}Fe_xO_{20}$ ($a \sim 2a_p\sqrt{2}$, $c \sim a_p$) has been determined from powder neutron diffraction data. This study shows that the substitution of iron for copper in the perovskite $La_{6.4}Sr_{1.6}Cu_8O_{20}$ does not influence the oxygen stoichiometry which remains fixed to "O_{20}". The singly substituted phase $La_{6.4}Sr_{1.6}Cu_{6.8}Fe_{1.2}O_{20}$ and the double-substituted phases $La_{6.4-x}Sr_{1.6+x}Cu_{8-x}Fe_xO_{20}$ (x = 1.2 and 2.0) are all characterized by a preferential occupation of the octahedral rows by Fe(III), whereas small amounts of Fe(III) are evidenced on the pyramidal sites. The examination of the interatomic distances also shows that the substitution of iron for copper tends to decrease the anisotropic character of the structure. One indeed observes that the (Cu,Fe)–O apical bonds of the flattened octahedra increase whereas the (Cu,Fe)–O equatorial bonds decrease as the Fe(III) content increases. Comparatively, the (Cu,Fe)–O apical bonds of the stretched pyramids decrease whereas the (Cu,Fe)–O equatorial bonds increase as the Fe(III) content increases.

Introduction

Substitution of iron for copper in cuprates related to the perovskite has been extensively studied these last years in order to understand relationships between magnetism and superconductivity. In this respect, the oxygen-deficient perovskite $(La,Sr)_8Cu_8O_{20}$[1] is of great interest although it does not superconduct. This good metallic conductor exhibits in fact a three-dimensional $[Cu_8O_{20}]_\infty$ framework, built up from rows of corner-sharing CuO_6 octahedra, CuO_5 pyramids, and CuO_4 planar groups running along the c axis of the tetragonal cell (Figure 1) so that units belonging to the superconducting "123" (e.g., $YBa_2Cu_3O_7$) and "2223" (e.g., $Tl_2Ba_2Ca_2Cu_3O_{10}$) or "1223" (e.g., $TlBa_2Ca_2Cu_3O_9$) structures can be recognized.

The study of the substitution of iron for copper in this structure has allowed two series of oxides to be isolated:[2] $La_{6.4}Sr_{1.6}Cu_{8-x}Fe_xO_{20}$ (singly substituted oxides) and $La_{6.4-x}Sr_{1.6+x}Cu_{8-x}Fe_xO_{20}$ (coupled substituted oxides). The two series differ by their homogeneity ranges $0 \le x \le 1.2$ and $0 \le x \le 2$, respectively, and by their electrical properties that remain metallic or semimetallic for the second series whereas it becomes semiconducting for the first one. The Mössbauer spectroscopy data[2] recorded for the composition $La_{4.4}Sr_{3.6}Cu_6Fe_2O_{20}$ (x = 2 in the coupled substituted series) showed an ordered distribution of iron in the structure, forming rows of corner-sharing FeO_6 octahedra. Nevertheless, a part of iron (about 15%) was found to exhibit the pyramidal coordination. At this stage two hypotheses can be proposed. The first one deals with a partial disordering of Fe(III) in the $[Cu_{8-x}Fe_xO_{20}]_\infty$ framework, so that about 15% of the original pyramidal sites would be occupied by iron. The second hypothesis deals with the appearance of oxygen vacancies in the octahedral rows, leading to the formation of additional pyramids, so that the framework would be formulated $[Cu_{8-x}Fe_xO_{20-y}]_\infty$. The powder X-ray diffraction investigation does not allow to decide between these two possibilities and the accuracy in the determination of the oxygen content by chemical analysis or TG measurement is not sufficient to detect small deviations from stoichiometry. To understand the physical properties of these cuprates, an accurate structure determination is absolutely necessary. For this, neutron diffraction is a helpful tool. We report herein on the powder neutron diffraction study of three compounds of these two series, the semiconducting $La_{6.4}Sr_{1.6}Cu_{6.8}Fe_{1.2}O_{20}$ and the metallic oxides $La_{5.2}Sr_{2.8}Cu_{6.8}Fe_{1.2}O_{20}$ and $La_{4.4}Sr_{3.6}Cu_6Fe_2O_{20}$.

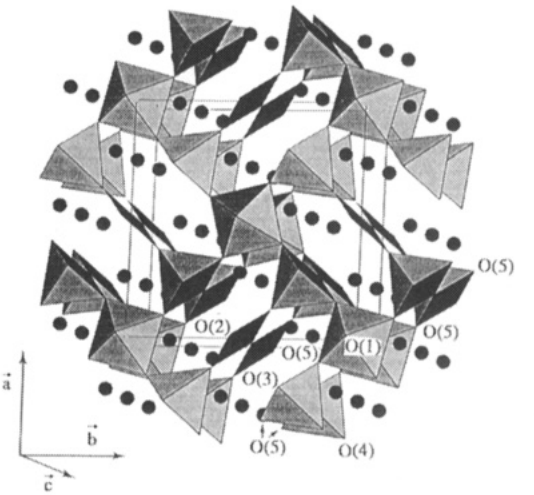

Figure 1. Perspective view of the structure of the tetragonal oxygen deficient perovskite $(La,Sr)_8Cu_8O_{20}$. The Cu_8O_{20} framework is drawn. Black circles represent the randomly distributed lanthanum and strontium atoms. Oxygen atoms are labeled.

[⊗] Abstract published in *Advance ACS Abstracts,* November 1, 1995.

(1) Er-Rakho, L.; Michel, C.; Raveau, B. *J. Solid State Chem.* **1988,** *73,* 514.

(2) Genouel, R.; Michel, C.; Nguyen, N.; Hervieu, M.; Raveau, B. *J. Solid State Chem.* **1995,** *115,* 469.

0897-4756/95/2807-2181$09.00/0

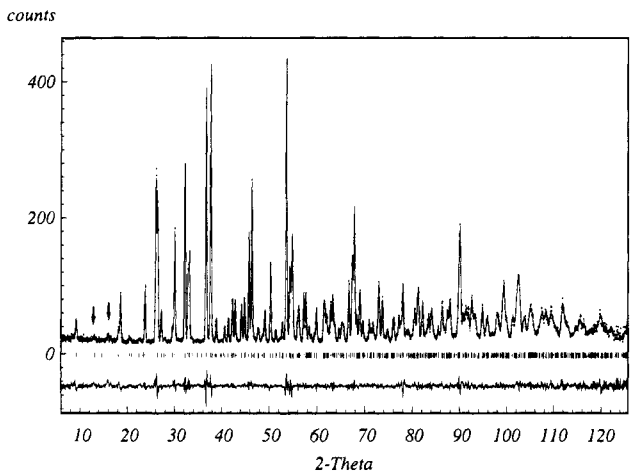

Figure 2. Experimental (dotted line) and calculated (solid line) neutron diffraction patterns of $La_{4.4}Sr_{3.6}Cu_6Fe_2O_{20}$. Small bars indicate the Bragg angles positions. At the bottom of the figure, the difference neutron pattern is plotted. Extrapeaks with regard to the $2a_p\sqrt{2} \times 2a_p\sqrt{2} \times c$ cell are indicated by arrows.

Experimental Section

Three nominal compositions were considered: $La_{6.4}Sr_{1.6}Cu_{6.8}Fe_{1.2}O_y$, $La_{5.2}Sr_{2.8}Cu_{6.8}Fe_{1.2}O_y$, and $La_{4.4}Sr_{3.6}Cu_6Fe_2O_y$. The first corresponds to the limit of iron substitution in the $La_{6.4}Sr_{1.6}Cu_{8-x}Fe_xO_{20}$ series, the second and third belong to the series $La_{6.4-x}Sr_{1.6+x}Cu_{8-x}Fe_xO_{20}$.

About 10 g of each composition were prepared from predried La_2O_3, CuO, Fe_2O_3, and $SrCO_3$ mixed in appropriate ratios according to the above formula. The mixtures were heated in air in a platinum crucible at 1000 °C for 24 h and then quenched down to room temperature. After regrinding, the thermal process was repeated once and the purity of the resulting powders was checked by X-ray diffraction.

Neutron diffraction data were collected at the laboratoire Léon Brillouin (Saclay, France) with the 3T2 diffractometer, from $2\theta = 6°$ to $2\theta = 126°$ by step scanning with increment of $0.05°(2\theta)$. The wavelength used was 1.2272 Å.

The oxygen content was determined by chemical analysis using a redox back-titration method. Tetravalent iron and trivalent copper species, if they exist, were reduced into Fe(III) and Cu(II) by a known amount of iron(II) chloride in acid solution. The amount of unreacted Fe(II) was then determined by titration with potassium dichromate. Chemical analysis revealed oxygen contents close to 20.0(1) whatever the composition (ranging from 19.9(1) to 20.0(1)).

Calculations were performed using the profile refinement computer program FULLPROF.[3] The following scattering amplitudes were used ($\times 10^{-12}$ cm): 0.772(Cu), 0.824 (La), 0.702 (Sr), 0.580(O), 0.954 (Fe).[4]

Results and Discussion

The X-ray diffraction patterns of the three samples do not reveal any impurity peaks with regard to the tetragonal symmetry, $a \sim 2a_p\sqrt{2}$, $c \sim a_p$, where a_p is the lattice constant of the cubic perovskite. However, two weak diffraction lines at $2\theta \sim 12.8°$ and 15.75°, which cannot be indexed with the above parameters, are observed on the neutron diffraction pattern (see arrows Figure 2). These extrapeaks could be indexed considering a doubling of the c parameter, as (111) and (021) reflections. The absence of superstructure reflections on the corresponding electron diffraction patterns[2] prevents consideration of a doubling of the nuclear cell but suggests that these extrapeaks could correspond to a magnetic ordering or to the presence of impurity. The magnetic susceptibility and Mössbauer measurements[2] showed a paramagnetic behavior above 300 K; in addition, no increase of the intensity of these lines can be observed for the pattern recorded at 10 K with respect to those recorded at 300 K; so that these peaks cannot be assigned to a magnetic contribution but are more probably due to an unknown phase, which is present at a level below the detection limits of the X-ray diffraction. They were omitted for the calculations. For the three samples $La_{6.4}Sr_{1.6}Cu_{6.8}Fe_{1.2}O_{20}$ and $La_{6.4-x}Sr_{1.6+x}Cu_{8-x}Fe_xO_{20}$ ($x = 1.2$ and 2.0), the starting model was that of the pristine compound $La_{8-x}Sr_xCu_8O_{20}$[1] (see Table 1). Calculations were made using the space group *P4/mbm*. Lanthanum and strontium were randomly distributed on equivalent positions (8*j* sites) with an occupancy factor corresponding to the nominal composition. Iron was located on 2(a) sites (0,0,0), i.e., on the octahedral site of the structure. For the composition $La_{4.4}Sr_{3.6}Cu_6Fe_2O_{20}$, location of iron on two different sites, octahedral and pyramidal, was considered; this model was deduced from previous Mössbauer spectroscopy results.[2] The oxygen stoichiometry was initially fixed to 20.

The profile parameters (background and shape parameters) and lattice constants were first refined. For the latter, the obtained values are given in Table 1. They are close to those refined from X-ray diffraction data[2] (a = 10.8072(6), 10.7930(6), and 10.7807(4) Å, and c = 3.8987(3), 3.8894(3), and 3.9026(1) Å, for $La_{6.4}Sr_{1.6}Cu_{6.8}Fe_{1.2}O_{20}$, $La_{5.2}Sr_{2.8}Cu_{6.8}Fe_{1.2}O_{20}$, and $La_{4.4}Sr_{3.6}Cu_6Fe_2O_{20}$, respectively), except for $La_{4.4}Sr_{3.6}Cu_6Fe_2O_{20}$ for which the neutron diffraction pattern has been recorded at 10 K. Positional parameters and then isotropic thermal factors were successively refined. In each case, the positional parameters remain close to those obtained from a powder neutron diffraction study[1] and a single-crystal X-ray diffraction study[5] of iron-free samples, and from a powder X-ray diffraction study of $La_{4.4}Sr_{3.6}Cu_6Fe_2O_{20}$.[2]

For each sample, the isotropic thermal factors for O(2) and O(3) are high compared to the other elements. The case of $La_{6.4}Sr_{1.6}Cu_{6.8}Fe_{1.2}O_{20}$ is a good example. $B_{O(2)}$ and $B_{O(3)}$ are found to be 2.5(2) and 1.7(1) Å^2, respectively, whereas all the other B values are lower than 1 Å^2. For these parameters, the profile and nuclear R factors are $R_p = 6.1\%$, $R_{wp} = 8\%$, $R_n = 7.7\%$. To explain these high values, two hypotheses can be considered: an atomic deficiency at the level of these sites or anisotropic thermal vibrations. Two features are in favor of the second hypothesis. The first deals with the fact that the B factors of O(2) and O(3) are considerably lowered for the pattern recorded at 10 K. The second concerns the Fourier map sections that show a non-spherical nuclear density distribution, but a disk shape distribution in the *ab* plane. For those two reasons anisotropic thermal coefficients were introduced for O(2) and O(3) in the calculations. The anisotropic temperature coefficients U_{ij} (Table 1) confirm that the thermal vibrations of O(2) and O(3) are significantly larger in

(3) Rodriguez-Carvajal, J.: Laboratoire Léon Brillouin, Saclay, Oct, 1994.

(4) Sears, V. F. *Thermal-Neutron Scattering Lengths and Cross Sections for Condensed Matter Research*; Chalk River Nuclear Laboratories, Chalk River Ontario, June, 1984.

(5) Lee, J. Y.; Kim, J. S.; Swinnea, J. S.; Steinfink, H. *J. Solid State Chem.* **1990**, *84*, 335.

Table 1. Variable Parameters and Reliability Factors after Refinement (S.G.: *P4/mbm*) (Numbers in Parentheses Are Standard Deviations)

formula		$La_{4.4}Sr_{3.6}Cu_6Fe_2O_{20}$				$La_{5.2}Sr_{2.8}Cu_{6.8}Fe_{1.2}O_{20}$				$La_{6.4}Sr_{1.6}Cu_{6.8}Fe_{1.2}O_{20}$			
site	atom	x	y	z	B (Å^2)	x	y	z	B (Å^2)	x	y	z	B (Å^2)
8(j)	La/Sr	0.2571(1)	0.4726(1)	0.5	0.28(2)	0.2585(1)	0.4710(1)	0.5	0.58(2)	0.2582(2)	0.4707(2)	0.5	0.76(4)
2(a)	Cu(1)/Fe(1)[a]	0	0	0	0.11(7)	0	0	0	0.23(4)	0	0	0	0.35(8)
2(d)	Cu(2)	0.5	0	0	0.09(7)	0.5	0	0	0.30(5)	0.5	0	0	0.42(9)
4(g)	Cu(3)/Fe(2)[a]	0.2251(1)	0.7251	0	0.28(4)	0.2225(1)	0.7225	0	0.41(3)	0.2202(2)	0.7202	0	0.38(5)
2(b)	O(1)	0	0	0.5	0.24(7)	0	0	0.5	0.59(7)	0	0	0.5	0.88(12)
2(c)	O(2)	0.5	0	0.5		0.5	0	0.5		0.5	0	0.5	
4(h)	O(3)	0.2202(2)	0.7202	0.5		0.2195(1)	0.7195	0.5		0.2198(3)	0.7198	0.5	
4(g)	O(4)	0.3768(2)	0.8768	0	0.44(5)	0.3768(2)	0.8768	0	0.76(5)	0.3754(3)	0.8754	0	0.97(8)
8(i)	O(5)	0.1569(2)	0.0962(2)	0	0.36(3)	0.1578(2)	0.0958(2)	0	0.68(3)	0.1611(3)	0.0928(3)	0	1.00(6)
	a (Å)			10.7480(3)				10.7870(3)				10.8088(5)	
	c (Å)			3.8976(2)				3.8915(1)				3.8992(2)	
	R_p (%)			5.44				3.84				5.86	
	R_{wp} (%)			6.47				4.71				7.60	
	R_n (%)			2.80				3.53				6.59	

site	atom	$U_{11} = U_{22}$	U_{33}	U_{12}	U_{eq}[b]	$U_{11} = U_{22}$	U_{33}	U_{12}	U_{eq}[b]	$U_{11} = U_{22}$	U_{33}	U_{12}	U_{eq}[b]
2(c)	O(2)	150(15)	117(14)	61(19)	139(14)	297(15)	43(11)	123(19)	212(13)	516(36)	67(24)	29(11)	367(32)
4(h)	O(3)	84(9)	11(7)	60(10)	60(8)	182(9)	41(6)	92(10)	135(8)	324(20)	78(13)	90(25)	242(17)

[a] Cu(1)/Fe(1) = 0.14/0.86 and Cu(3)/Fe(2) = 0.93/0.07 in $La_{4.4}Sr_{3.6}Cu_6Fe_2O_{20}$. [b] U_{eq} was calculated from $^1/_3[(2U_{11}) + U_{33}]$. $U_{13} = U_{23} = 0$, all U values are $\times 10^{-4}$ Å^2.

Table 2. Interatomic Distances (Å) Compared to Those Observed in the Iron-Free Sample[1]

M–O (Å)	$La_{4.4}Sr_{3.6}Cu_6Fe_2O_{20}$	$La_{5.2}Sr_{2.8}Cu_{6.8}Fe_{1.2}O_{20}$	$La_{6.4}Sr_{1.6}Cu_{6.8}Fe_{1.2}O_{20}$	$La_{6.4}Sr_{1.6}Cu_8O_{20}$
La/Sr–O(1) × 1	2.628(2)	2.624(2)	2.636(3)	2.602(3)
La/Sr–O(2) × 1	2.778(2)	2.805(2)	2.805(3)	2.862(3)
La/Sr–O(3) × 1	2.690(3)	2.709(2)	2.715(5)	2.730(4)
La/Sr–O(3) × 1	2.724(3)	2.728(2)	2.733(5)	2.747(4)
La/Sr–O(4) × 2	2.633(2)	2.636(2)	2.636(3)	2.645(3)
La/Sr–O(5) × 2	2.533(2)	2.532(2)	2.511(3)	2.511(3)
La/Sr–O′(5) × 2	2.867(2)	2.862(2)	2.904(3)	2.848(3)
octahedra				
Cu(1)/Fe(1)–O(1) × 2	1.949(1)	1.946(1)	1.950(1)	1.932(1)
Cu(1)/Fe(1)–O(5) × 4	1.978(2)	1.999(2)	2.010(4)	2.038(4)
square plane				
Cu(2)–O(2) × 2	1.949(1)	1.946(1)	1.950(1)	1.932(1)
Cu(2)–O(4) × 2	1.872(2)	1.882(2)	1.905(4)	1.906(4)
square pyramids				
Cu(3)/Fe(2)–O(3) × 2	1.950(1)	1.946(1)	1.950(1)	1.932(1)
Cu(3)/Fe(2)–O(4) × 1	2.307(3)	2.354(3)	2.372(4)	2.395(4)
Cu(3)/Fe(2)–O(5) × 2	1.878(3)	1.880(2)	1.882(4)	1.860(4)

the ab plane than along the c axis in agreement with the previous single-crystal X-ray diffraction study of $La_{6.16}Sr_{1.84}Cu_{7.66}O_{20}$.[5] With this model, the R factors could be lowered to $R_p = 5.9\%$, $R_{wp} = 7.6\%$, $R_n = 6.6\%$, without any significant change for the other variable parameters. Refinement of the occupancy factors of O(2) and O(3) sites led to deviations from a full occupation lower than the estimated standard deviations (0.98(3) for O(2) and 0.99(3) for O(3)) and could not be considered as significant. The same feature was observed for the two other compositions.

The final atomic parameters are given in Table 1 for the three samples, and as an example the experimental and difference neutron diffraction patterns are plotted in Figure 2 for $La_{4.4}Sr_{3.6}Cu_6Fe_2O_{20}$. One observes that the B factors of the O(1) and O(5) atoms, that correspond to the apical and equatorial oxygen atoms of the octahedra respectively are reasonably low, ranging from 0.24 to 1 Å;[2] all attempts to refine the occupancy of these oxygen sites led to a full occupation. In the same way, Fourier map sections at the level of a possible supplementary oxygen site (4(g): x, $^1/_2 + x$, 0 with $x \sim 0.125$), inside the hexagonal tunnels, which would involve an oxygen excess, did not reveal any significant nuclear density. This was confirmed by the calculations performed with this hypothesis which led to a slightly negative occupancy factor for this site.

These results definitely show that the introduction of iron in the $(La,Sr)_8Cu_8O_{20}$ cuprate does not influence the oxygen stoichiometry, which remains unchanged corresponding to "O_{20}". Consequently it can be stated that the two different coordinations of iron observed from Mössbauer spectroscopy for $La_{4.4}Sr_{3.6}Cu_6Fe_2O_{20}$[2] correspond to a preferential occupation of the octahedral rows (Cu(1) sites: 86% of the total iron content) and a minor occupation of the pyramidal rows by iron (Cu(3) sites: 14% of the total iron content), without any formation of new pyramidal sites from the Cu(1) octahedra. This is confirmed by the refinement of the occupancy factors of these two sites which shows that the 2(a) Cu(1) site is 90% occupied by iron (i.e., 90% of the total iron content), whereas the 4(g) Cu(3) site is 5% occupied (i.e., 10% of the total iron content); nevertheless the rather small difference between the scattering amplitudes of Cu and Fe of about 20%, leads to a large standard deviation (6%), which implies that the Mössbauer results must be considered as more accurate.

The interatomic distances compared to those of the pristine $La_{6.4}Sr_{1.6}Cu_8O_{20}$ phase are listed in Table 2. It is remarkable that the Jahn–Teller effect of copper in

this structural type is different from that observed in superconducting layered cuprates, since the CuO_6 octahedra are flattened, i.e., compressed along $\vec{c}$, with four long equatorial (Cu,Fe)−O distances and two short apical (Cu,Fe)−O distances. On the opposite the CuO_5 pyramids are similar to those observed in the superconducting cuprates with four short (Cu,Fe)−O basal distances and one longer apical (Cu,Fe)−O bond in the *ab* plane. Clearly the pristine cuprate is the most anisotropic; it exhibits infinite "Cu−O−Cu" chains running along $\vec{c}$ characterized by Cu−O bonds of 1.932 Å, whereas the infinite zigzag "Cu−O−Cu" chains running along ⟨110⟩ are built from two short Cu(3)−O(5) bonds (1.86 Å) that alternate with two long Cu(1)−O(5) bonds (2.03 Å) according to the sequence "O(5)−Cu(3)−O(5)−Cu(1)−O(5)". The substitution of iron for copper decreases significantly this anisotropy. This is clearly observed for the $(Cu,Fe)O_6$ octahedra (Table 2) in which the introduction of iron tends to decrease the equatorial distances and to increase the apical ones. This is confirmed by the ratio $d(Cu-O)_{a_p}/d(Cu-O)_{e_q}$ that increases from 0.948 for $La_{6.4}Sr_{1.6}Cu_8O_{20}$ to 0.985 for $La_{4.4}Sr_{3.6}Cu_6Fe_2O_{20}$. This feature is in agreement with the fact that iron, which does not exhibit the Jahn−Teller effect, substitutes for Cu(1), leading to more regular octahedra. It also explains the decrease of the *a* parameter and the increase of the *c* parameter with the increase of the Fe content in both series.[2] In the same way, the introduction of Fe(III) on the Cu(3) pyramidal site leads to an increase of the equatorial (Cu,Fe)−O distances and to a decrease of the apical (Cu,Fe)−O bond (Table 2). This is in perfect agreement with the fact that for trivalent iron in square-pyramidal coordination, the apical Fe−O distance is significantly shorter than the equatorial distances as shown from the ratio $d(Fe-O)_{a_p}/d(Fe-O)_{e_q}$ for $Sr_3Fe_2O_6$ (0.952),[6] $YBa_2Fe_3O_8$ (0.929),[7] $YBaCuFeO_5$ (0.963),[8] contrary to copper square pyramids which always exhibits a ratio larger than unity: $La_2SrCu_2O_6$ (1.14),[9] $La_{1.9}Ca_{1.1}Cu_2O_6$ (1.205),[10] $YBa_2Cu_3O_6$ (1.274),[11] $YBaCuFeO_5$ (1.135),[8] $La_{6.4}Sr_{1.6}Cu_8O_{20}$ (1.263).[1] In our phases, this ratio remains larger than 1 (1.238, 1.231, and 1.205 for $La_{6.4}Sr_{1.6}Cu_{6.8}Fe_{1.2}O_{20}$, $La_{5.2}Sr_{2.8}Cu_{6.8}Fe_{1.2}O_{20}$, and $La_{4.4}Sr_{3.6}Cu_6Fe_2O_{20}$, respectively) due to the fact that only a small amount of Fe(III) can be substituted for copper on the Cu(3) pyramidal site. For a same iron content, the copper (iron)−oxygen distances are slightly lower in $La_{5.2}Sr_{2.8}Cu_{6.8}Fe_{1.2}O_{20}$ with respect to $La_{6.4}Sr_{1.6}Cu_{6.8}Fe_{1.2}O_{20}$ despite the increase of the mean size of the atoms sitting in the hexagonal tunnels. This result agrees with the assumption that formally trivalent copper content is higher in the $La_{6.4-x}Sr_{1.6+x}Cu_{8-x}Fe_xO_2$ series than in the $La_{6.4}Sr_{1.6}Cu_{8-x}Fe_xO_{20}$ series and confirms that they can be described by the formulas $La_{6.4-x}Sr_{1.6+x}Cu^{II}_{6.4-x}Cu^{III}_{1.6}Fe^{III}_xO_{20}$ and $La_{6.4}Sr_{1.6}Cu^{II}_{6.4}Cu^{III}_{1.6-x}Fe^{III}_xO_{20}$.

Taking into consideration the mixed valence Cu(II)−Cu(III) as repesentative of the electronic delocalization in the structure, which is also favored by the decrease of the Cu−O distances, this confirms the previous statements[2] according to which the hole carrier density is dramatically lower for $La_{6.4}Sr_{1.6}Cu^{II}_{6.4}Cu^{III}_{0.4}Fe^{III}_{1.2}O_{20}$ than in the oxides $La_{6.4-x}Sr_{1.6+x}Cu^{II}_{6.4-x}Cu^{III}_{1.6}Fe^{III}_xO_{20}$, explaining that the first one exhibits a semiconducting behavior whereas the oxides of the second series are metallic or semimetallic. In the previous study of the electron-transport properties of the oxides of the second series, an increase of the conductivity of these compounds was observed by annealing the samples in oxygen. This phenomenon was interpreted as the existence, for the quenched samples, of oxygen deficiency according to the formula $La_{6.4-x}Sr_{1.6+x}Cu^{II}_{6.4-x}Cu^{III}_{1.6}Fe^{III}_xO_{20-\epsilon}$. Another possibility is to envisage the introduction of oxygen bridging Cu(2) and Cu(3) in the oxygen annealed samples. In the studied compounds, the Cu(2)−Cu(3) distances (3.36−3.42 Å) are too short to allow oxygen to be inserted between these two copper atoms. Introduction of oxygen would imply an increase of the Cu(2)−Cu(3) distance and consequently an increase of the *a* parameter. The experimental *a* parameter of the oxygen-annealed compounds tend to be slightly smaller than that of the quenched samples. This feature disagrees with a possible overstoichiometry.

Concluding Remarks

The neutron diffraction study of the oxygen deficient perovskites $(La, Sr)_8Cu_{8-x}Fe_xO_{20}$ definitely shows the high stability of the oxygen framework which is not influenced by iron substitution and remains fixed to "O_{20}". This study demonstrates clearly that iron occupies preferentially the octahedral sites of the structure and that the two different coordinations observed for iron in $La_{4.4}Sr_{3.6}Cu_6Fe_2O_{20}$ from Mössbauer spectroscopy is not the consequence of an oxygen deficiency over the O(1) sites but is due to a partial disordering of iron over two different cristallographic sites (octahedral and pyramidal). It also shows that the introduction of iron modifies significantly the metal−oxygen distances in the $Cu_{8-x}Fe_xO_2$ framework leading to a decrease of the anisotropy of the structure. These modifications contribute to the evolution of the transport properties of the materials.

Acknowledgment. The authors gratefully acknowledge Dr. Francoise Bouree of Laboratoire Leon Brillouin, Saclay, France, for her helpful collaboration in recording the powder neutron diffraction data.

CM950260T

(6) Dann, S.; Weller, M. T.; Currie, D. B. *J. Solid State Chem.* **1992**, *97*, 179.
(7) Huang, Q.; Karen, P.; Karen, V. L.; Kjekshus, A.; Lynn, J. W.; Rosov, N.; Santoro, A. *Phys. Rev. B* **1992**, *45*, 9611.
(8) Caignaert, V.; Mirabeau, I.; Bouree, F.; Nguyen, N.; Ducouret, A.; Greneche, J. M.; Raveau, B. *J. Solid State Chem.* **1995**, *114*, 24.
(9) Caignaert, V.; Nguyen, N.; Raveau, B. *Mater. Res. Bull.* **1990**, *25*, 199.
(10) Izumi, F.; Takayama-Muromachi, E.; Nakay, Y.; Asano, H. *Physica C* **1989**, *157*, 89.
(11) Roth, G.; Renker, B.; Heger, G.; Hervieu, M.; Domengès, B.; Raveau, B. *Z. Phys. B* **1987**, *69*, 53.